

Adiabatically twisting a magnetic molecule to generate pure spin currents in graphene

Firoz Islam and Colin Benjamin*

National institute of Science education & Research, Bhubaneswar 751005, India

The spin orbit effect in graphene is too muted to have any observable significance with respect to its application in spintronics. However, graphene technology is too valuable to be rendered impotent to spin transport. In this communication we look at the effect of adiabatically twisting a single molecule magnet embedded in a graphene monolayer. Surprisingly, we see that pure spin currents (zero charge current) can be generated from the system via quantum pumping. In addition we also see spin selective current can also be pumped from the system. The pure spin current seen is quite resilient to temperature while disorder has a limited effect. Further the direction of these spin pumped currents can be easily and exclusively controlled by the magnetization of the single molecule magnet with disorder having no effect on the magnetization control of the pumped spin currents.

I. INTRODUCTION

Graphene has been a revolutionary material of this the 21st century. Its remarkable that since its discovery around a decade ago it has captured the interest of the scientific community in ways that even High Tc superconductors in its hey days couldn't. A cursory look at graphenes properties would provide reasons for this. Graphene is light with huge tensile strength and crucially in contrast to most materials, electronic energy is linearly proportional to its wave vector and not its square and it shows quite remarkable quantum phenomena like Klein tunneling[1] and room temperature quantum Hall effect[2], etc. Notwithstanding the many advantages of using graphene to transport electrons faster and with less dissipation it has been observed that spin orbit effect in graphene is at best negligible thus making them of no practical use for applications in spintronics. Then how do we exploit the manifest advantages of graphene and marry them to spintronics. In this communication we address this issue. We intend to embed a monolayer of Graphene with a single molecule magnet. We then adiabatically modulate two independent parameters of the resulting system to pump a pure spin current. The two parameters we modulate are one- the Magnetization strength of the magnetic molecule which has been shown to be controlled by twisting it[3]. Secondly, we add a delta function like point interaction, which can either be an isolated adatom in the Graphene monolayer or an extended line defect or even a very thin potential barrier with the strength of the potential barrier being controlled by a gate voltage. Using these two parameters we intend to pump a pure spin current.

Adiabatic quantum pumping is a means of transferring charge and/or spin carriers without applying any external perturbation (like voltage bias, etc.) by the cyclic variation of two independent system parameters. The theory of adiabatic quantum pumping was developed in 1998[4] based on the fact that adiabatic modulations to a 2DEG can lead to changes in local density of states and thus current transport. In 1999, an adiabatic quantum electron pump was reported in an open quantum dot where the pumping signal was produced in response to the cyclic deformation of the confining potential[5]. The variation

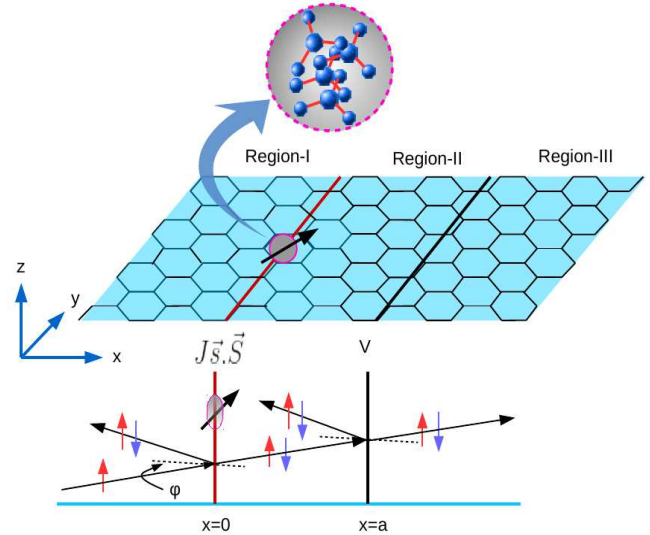


Figure 1. A single molecule magnet at $x = 0$ is adiabatically twisted along with an electrostatic delta potential at $x = a$ to generate pure spin currents in graphene.

of the dot's shape changes electronic quasi energy states of the dot thus 'pumping' electrons from one reservoir to another. The AC voltages applied to the quantum dot in order to change the shape result in a DC current when the reservoirs are in equilibrium. This non-zero current is only produced if there are at least two time varying parameters in the system as a single parameter quantum pump does not transfer any charge. Later on the study of adiabatic pumping phenomenon has been extended to adiabatic spin pumping both in experiment as well as theory[6, 7]. In the experiment on quantum spin pumping one generates a pure spin current via a quantum dot by applying an in plane magnetic field which is adiabatically modulated to facilitate a net transfer of spin. Many spintronic devices, such as the spin valve and magnetic tunneling junctions[8], are associated with the flow of spin polarized charge currents. Spin polarized currents coexist with charge currents and are generated when an imbalance between spin up and spin down carriers is created, for example, by using magnetic materials or applying a strong magnetic field or by exploiting spin-orbit cou-

* cbiop@yahoo.com

pling in semiconductors[8]. The spin transport aided by bias voltage have been studied earlier[9–11].

More recently, there has been an increasing interest in the generation of pure spin current by quantum pumping without an accompanying charge current[6]. In monolayer graphene, a group has attempted to address this issue by proposing a device, consisting of ferromagnetic strips and gate electrodes[12]. However, ferromagnetic strips in graphene are unwieldy and lead to further complication as spin polarization is lost at the ferromagnet-graphene interface. In this work we look at only a piece of monolayer graphene without any ferromagnets but with two impurities one magnetic(SMM) the other non-magnetic. Independently modulating these two we show generation of pure spin currents. The generation of a pure spin-current is only possible if all spin-up electrons flow in one direction and equal amount of spin-down electrons flow in the opposite direction. In this case the net charge current $I_{charge} = I_{\uparrow} + I_{\downarrow}$ vanishes while a finite spin current $I_{spin} = I_{\uparrow} - I_{\downarrow}$ exists, because $I_{\uparrow} = -I_{\downarrow}$, where I_{\uparrow} or I_{\downarrow} are the electron current with spin-up or spin-down. Further we also see generation of spin selective currents namely either only I_{\uparrow} or I_{\downarrow} and this implies the total magnitude of charge current is identical to that of the spin current.

In this work we show how pure spin currents and spin selective currents can be generated via twisting a single molecule magnet. Single molecule magnets are of great importance for molecular spintronics. Such molecules can now be synthesized, for example the molecule $Mn_{12}ac$, which has a ground state with a large spin ($S=10$), and a very slow relaxation of magnetization at low temperature[13]. SMM's do not just have integer spin values a number of SMM's like Mn_4O_3 complex[14] have large half integer spin $S = 9/2$. However, in a literal twist to this tale (pun intended), a few years back scientists revealed that these big spin molecules can be twisted and thus their magnetization can be easily altered [15]. This fact we utilize in our adiabatic pumping mechanism. The mechanism of twisting is not difficult to implement. SMM's have a metallic core (for example in Mn_{12} complexes the metallic core consists of the $Mn-O-N-Mn$ moiety) and a deliberate targeted structural distortion of it leads to change in the magnetization of the SMM so much so that a initially ferromagnetic SMM can undergo a twist to a anti-ferromagnetic SMM. The twist can be effectively controlled by two methods-(i) A simple substitution of one type of atom (in Mn_{12} complexes a H atom) by another sterically demanding atom (again in Mn_{12} complexes by a Me, Et, Ph, etc. atom) or by (ii) the other way this can be achieved is through the use of hydrostatic pressure[16]. In this method external hydrostatic pressure is applied on the SMM leading to a twisting of the metallic core and thus a net change in magnetization. While the substitution method leads to a discrete change in the magnetization the pressure method leads to a continuous change. Therefore, the pressure method is much more amenable to the quantum pumping mechanism wherein the pressure applied could be continuously changed albeit adiabatically leading to a adiabatic change in magnetization and thus the exchange interaction J .

II. THEORY

Graphene is a monatomic layer of graphite with a honeycomb lattice structure [18] that can be split into two triangular sublattices A and B . The electronic properties of graphene are effectively described by the massless Dirac equation. The presence of isolated Fermi points, K and K' , in its spectrum, gives rise to two distinctive valleys. We consider a sheet of graphene on the x - y plane. In Fig. 1 we sketch our proposed system. For a quantitative analysis we describe our system by the massless Dirac equation in presence of an embedded single magnetic molecule(SMM). The Hamiltonian used to describe a SMM has the following terms:

$$H_{SMM} = -DS_z^2 - Js.S \quad (1)$$

The first term represents the Energy of the SMM. D is an uniaxial anisotropy constant and S_z is the z component of the spin of the Molecular magnet. The second term is most relevant to us since we deal with electron transport. The Dirac electrons in graphene interact with SMM only via the exchange term $-Js.S$. Further the magnitude in realistic SMM of D is very small as compared to J , $D = 0.292 Kelvin = 0.025$ meV while $J = 100$ meV almost a thousand times larger[17]. Though anisotropy is very important term in preserving the intrinsic properties of SMM, it's effect on conduction electron is hardly a small correction to energy, nothing else. The first term will only be relevant in electronic structure calculations for electronic transport calculations it is not relevant and the only term of interest in the exchange coupling. Thus we only consider the second term in the subsequent analysis. We consider a single molecule magnet at $x = 0$ and another electrostatic delta potential at $x = a$ nm. The Hamiltonian of a Dirac electron moving along x -direction can be written as

$$H = \hbar v_F \sigma \cdot \mathbf{p} + Js.S\delta(x) + V\delta(x-a). \quad (2)$$

The first term represent the kinetic energy term for graphene with σ the Pauli matrices that operate on the sub-lattices A or B and $\mathbf{p} = (p_x, p_y)$ the 2D momentum vector, second term is electron interacting with single molecule magnet and third term is an electrostatic delta potential. In the second term J represents the exchange interaction which depends on the magnetization of the SMM and twisting the SMM changes the magnetization thus effectively changing J . s represents the spin of the Dirac electron while S represents spin of the SMM. V represents strength of the adatom situated at a distance a from SMM. Here \hbar, v_F (set equal to unity hence forth) are the Planck's constant and the energy independent Fermi velocity for graphene. Eq. 2 is valid near the valley K in the Brillouin zone and $\Psi = [\psi_K^A(\mathbf{r}), \psi_K^B(\mathbf{r})]$ is a spinor containing the electron fields in each sublattice. The Hamiltonian for K' -valley can be obtained by replacing p_y by $(-p_y)$ in Eq. (2). Because of this symmetry i.e; $H_K(p_y) = H_{K'}(-p_y)$, transport coefficients will be same in both valleys. So we are confining our discussion only in K -valley.

To calculate the quantum spin pumped currents we need to introduce the basic theory of quantum pumping which is quite

well known as well as solve the scattering problem for electron with spin (up or down) incident from either left or right. We introduce them below:

A. Quantum pumped currents

To calculate quantum pumped currents we proceed as follows: Thus charge passing through lead μ - to the left of Molecular magnet, due to infinitesimal change of system parameters is given by-

$$dQ_{\sigma\mu}(t) = e \left[\frac{dN_{\sigma\mu}}{dX_1} \delta X_1(t) + \frac{dN_{\sigma\mu}}{dX_2} \delta X_2(t) \right] \quad (3)$$

with the spin current transported in one period being-

$$I_{\sigma\mu} = \frac{ew}{2\pi} \int_0^\tau dt \left[\frac{dN_{\sigma\mu}}{dX_1} \frac{dX_1}{dt} + \frac{dN_{\sigma\mu}}{dX_2} \frac{dX_2}{dt} \right] \quad (4)$$

In the above $\tau = 2\pi/w$ is the cyclic period. The quantity $dN_{\sigma\mu}/dX_i$ is the emissivity which is determined from the elements of the scattering matrix, in the zero temperature limit by -

$$\frac{dN_{\sigma\mu}}{dX_i} = \frac{1}{2\pi} \sum_{\sigma'} \Im \left(\frac{\partial s_{\mu\nu}^{\sigma\sigma'}}{\partial X_i} s_{\mu\nu}^{\sigma\sigma'} \right) \quad (5)$$

Here $s_{\mu\nu}^{\sigma\sigma'}$ denote the elements of the scattering matrix as denoted above, as evident μ, ν and i can only take values 1,2, while σ, σ' takes values \uparrow and \downarrow depending on whether spin is up or down. The symbol “ \Im ” represents the imaginary part of the complex quantity inside parenthesis.

The spin pump we consider is operated by adiabatically twisting the magnetic molecule thus modulating the magnetic interaction between the magnetic molecule and scattered electrons “J” and the strength of the “delta” function potential V, herein $X_1 = J = J_0 + J_p \sin(\omega t)$ and $X_2 = V = V_0 + V_p \sin(\omega t + \theta)$. A paragraph on the experimental feasibility of the proposed device is given above the conclusion. As the pumped current is directly proportional to w (the pumping frequency), we can set it to be equal to 1 without any loss of generality.

By using Stoke's theorem on a two dimensional plane, one can change the line integral of Eq. (4) into an area integral, see for details Ref.6-

$$I_{\sigma\mu} = e \int_A dX_1 dX_2 \left[\frac{\partial}{\partial X_1} \frac{dN_{\sigma\mu}}{dX_2} - \frac{\partial}{\partial X_2} \frac{dN_{\sigma\mu}}{dX_1} \right] \quad (6)$$

Substitution of Eq. (5) into Eq. (6) leads to,

$$I_{\sigma\mu} = e \int_A dX_1 dX_2 \sum_{\sigma'=\uparrow,\downarrow; \nu=1,2} \Im \left(\frac{\partial s_{\mu\nu}^{\sigma\sigma'}}{\partial X_1} \frac{\partial s_{\mu\nu}^{\sigma\sigma'}}{\partial X_2} \right) \quad (7)$$

This current is for a particular angle of incidence (ϕ), as the scattering amplitudes depend on ϕ . So hereafter, we replace

$I_{\sigma\mu}$ by $I_{\sigma\mu}(\phi)$. If the amplitude of oscillation is small, i.e., for sufficiently weak pumping ($\delta X_i \ll X_i$), we have,

$$I_{\sigma\mu}(\phi) = \frac{ew\delta X_1 \delta X_2 \sin(\theta)}{2\pi} \sum_{\nu=1,2} \Im \left(\frac{\partial s_{\mu\nu}^{\sigma\sigma'}}{\partial X_1} \frac{\partial s_{\mu\nu}^{\sigma\sigma'}}{\partial X_2} \right) \quad (8)$$

In the considered case of a magnetic molecule and delta function potential the case of very weak pumping is defined by: $x_p \ll J_0 = V_0$, and Eq. 8 becomes-

$$I_{\sigma\mu}(\phi) = I_0 \sum_{\sigma'=\uparrow,\downarrow; \nu=1,2} \Im \left(\frac{\partial s_{\mu\nu}^{\sigma\sigma'}}{\partial J} \frac{\partial s_{\mu\nu}^{\sigma\sigma'}}{\partial V} \right) \quad (9)$$

wherein,

$$I_0 = \frac{ewx_p^2 \sin(\theta)}{2\pi}$$

As we consider only the pumped currents into lead 1(left of magnetic molecule), therefore $\mu = 1$. Further we drop the μ index in expressions below.

For weak pumping, we have the total pumped up-spin current given as follows:

$$I_\uparrow(\phi) = I_0 \left[\Im \left(\frac{\partial s_{11}^{\uparrow\uparrow*}}{\partial V} \frac{\partial s_{11}^{\uparrow\uparrow}}{\partial J} \right) + \Im \left(\frac{\partial s_{11}^{\uparrow\downarrow*}}{\partial V} \frac{\partial s_{11}^{\uparrow\downarrow}}{\partial J} \right) + \Im \left(\frac{\partial s_{12}^{\uparrow\uparrow*}}{\partial V} \frac{\partial s_{12}^{\uparrow\uparrow}}{\partial J} \right) + \Im \left(\frac{\partial s_{12}^{\uparrow\downarrow*}}{\partial V} \frac{\partial s_{12}^{\uparrow\downarrow}}{\partial J} \right) \right]. \quad (10)$$

Similarly, we can calculate the spin down current for the case of weak pumping by replacing $\uparrow \rightarrow \downarrow$ and vice-versa.

For strong pumping, we have the total up-spin current given as:

$$I_\uparrow = \frac{ew}{2\pi} \int_0^\tau dt \left[\frac{dN_\uparrow}{dX_1} \frac{dX_1}{dt} + \frac{dN_\uparrow}{dX_2} \frac{dX_2}{dt} \right], \text{ with} \\ \frac{dN_{\sigma\mu}}{dX_i} = \frac{1}{2\pi} \left[\Im \left(\frac{\partial s_{11}^{\uparrow\uparrow}}{\partial X_i} s_{11}^{\uparrow\uparrow*} \right) + \Im \left(\frac{\partial s_{11}^{\uparrow\downarrow}}{\partial X_i} s_{11}^{\uparrow\downarrow*} \right) + \Im \left(\frac{\partial s_{12}^{\uparrow\uparrow}}{\partial X_i} s_{12}^{\uparrow\uparrow*} \right) + \Im \left(\frac{\partial s_{12}^{\uparrow\downarrow}}{\partial X_i} s_{12}^{\uparrow\downarrow*} \right) \right]. \quad (11)$$

here we have dropped the lead index since we pump always to left lead (left to SMM) and $s_{\mu\nu}^{\sigma\sigma'}$ is complex conjugate of $s_{\mu\nu}^{\sigma\sigma'}$. To obtain the total current, we integrate over ϕ . Then the total spin-up pumped current for both weak as well as strong pumping becomes:

$$I_\uparrow = \int_{-\pi/2}^{\pi/2} I_\uparrow(\phi) \cos(\phi) d\phi. \quad (12)$$

Similarly, we can calculate the spin down current for the case of weak pumping by replacing $\uparrow \rightarrow \downarrow$ and vice-versa. In the above equations the scattering amplitudes represent- $s_{11}^{\uparrow\uparrow} = r_\uparrow$, reflection amplitude when spin-up electron is coming from the left side and reflected to the spin-up state.

$s_{11}^{\uparrow\downarrow} = r'_{\uparrow}$, reflection amplitude when spin-down electron is coming from the left side and reflected to the spin-up state
 $s_{12}^{\uparrow\uparrow} = t_{\uparrow}$, transmission amplitude when spin-up electron is coming from the right side and transmitted to the spin-up state.
 $s_{12}^{\uparrow\downarrow} = t'_{\uparrow}$, transmission amplitude when spin-down electron is coming from the right side and transmitted to the spin-up state.
 Numerically, we have calculated r_{\uparrow} , r'_{\uparrow} , t_{\uparrow} and t'_{\uparrow} and substituted in the above expression to obtain the spin-up pumping current.

Effect of finite temperature: So far our discussion is for zero temperature. The temperature effects could be easily captured by multiplying a factor $[-df(E)/dE]$ with pumping current and integrating over energy of incident electron[19] i.e;

$$I_{\sigma} = \int_{-\pi/2}^{\pi/2} \int_0^{\infty} \left[-\frac{df(E)}{dE} \right] I_{\sigma}(\phi) \cos(\phi) dE d\phi, \sigma = \uparrow, \downarrow. \quad (13)$$

where $f(E)$ is the Fermi-Dirac distribution function.

B. Solving the scattering problem

Let us consider an incident spin-up electron from left of magnetic molecule ($x < 0$) with energy E . The electron can be reflected or transmitted to spin-up/down state. Then the spinors, for the angle of incidence ϕ , in the various regions are given as:

Region-I ($x < 0$):

$$\Psi_A^I(x) = \begin{bmatrix} (e^{ikx} + r_{\uparrow} e^{-ikx})\chi_m \\ r_{\downarrow} e^{-ikx}\chi_{m+1} \end{bmatrix} \quad (14)$$

$$\Psi_B^I(x) = \begin{bmatrix} (e^{ikx+i\phi} - r_{\uparrow} e^{-ikx-i\phi})\chi_m \\ -r_{\downarrow} e^{-ikx-i\phi}\chi_{m+1} \end{bmatrix} \quad (15)$$

Region-II ($0 < x < a$):

$$\Psi_A^{II}(x) = \begin{bmatrix} (a_{\uparrow} e^{ikx} + b_{\uparrow} e^{-ikx})\chi_m \\ (a_{\downarrow} e^{ikx} + b_{\downarrow} e^{-ikx})\chi_{m+1} \end{bmatrix} \quad (16)$$

$$\Psi_B^{II}(x) = \begin{bmatrix} (a_{\uparrow} e^{ikx+i\phi} - b_{\uparrow} e^{-ikx-i\phi})\chi_m \\ (a_{\downarrow} e^{ikx+i\phi} - b_{\downarrow} e^{-ikx-i\phi})\chi_{m+1} \end{bmatrix} \quad (17)$$

and in Region-III ($x > a$):

$$\Psi_A^{III}(x) = \begin{bmatrix} t_{\uparrow} e^{ikx}\chi_m \\ t_{\downarrow} e^{ikx}\chi_{m+1} \end{bmatrix} \quad (18)$$

$$\Psi_B^{III}(x) = \begin{bmatrix} t_{\uparrow} e^{ikx+i\phi}\chi_m \\ t_{\downarrow} e^{ikx+i\phi}\chi_{m+1} \end{bmatrix}. \quad (19)$$

In the above equations, \uparrow and \downarrow stand for spin-up and spin-down electron. Here, $r_{\uparrow}, r_{\downarrow}$ and $t_{\uparrow}, t_{\downarrow}$ are the reflection and transmission amplitudes respectively. Also,

$k = E_F \cos(\phi)$ with $E_F (> 0)$ being the Fermi energy. χ 's denote the eigen states of S_z the z-component of spin operator for SMM, $S_z \chi_m = m \chi_m$ with m being the corresponding eigen value. The scattering is elastic and the exchange interaction conserves the z-component of the total spin $S + s$. The exchange operator in the Hamiltonian, $s \cdot \mathbf{S} = s_z S_z + (1/2)(s^- S^+ + s^+ S^-)$ acts as a spin-flipper for electrons with different values of s_z to those of S_z while for same values it acts as a normal barrier. $s^- S^+ \begin{bmatrix} 1 \\ 0 \end{bmatrix} \chi_m = F \begin{bmatrix} 0 \\ 1 \end{bmatrix} \chi_{m+1}$ and $s^+ S^- \begin{bmatrix} 0 \\ 1 \end{bmatrix} \chi_m = F' \begin{bmatrix} 1 \\ 0 \end{bmatrix} \chi_{m-1}$ with $F = \sqrt{(S-m)(S+m+1)}$ and $F' = \sqrt{(S+m)(S-m+1)}$. Here, $s^{\pm} = s_x \pm s_y$ and $S^{\pm} = S_x \pm S_y$ are the raising and lowering operators.

In solving the scattering problem from a delta potential the following two boundary conditions have to be met: i) continuity of the wave functions at the boundary and ii) discontinuity of the energy at the boundary. However, these boundary conditions work only if the system is described by the Schrodinger equation, but does not work for Dirac material like graphene. For Dirac equation, the wave functions on either side of delta potential are not continuous across the boundary.

At $x=0$, while taking integration on the both sides of the Dirac equations, $H\psi = E\psi$, one is stuck at the following integration:

$$\bar{\psi}(0) = \int_{x=0^-}^{x=0^+} \psi \delta(x) dx \quad (20)$$

because of the discontinuity of wave functions at the boundary. However, there is a standard way to avoid this difficulty, which has been widely used by many authors, by taking the average, i.e.,

$$\bar{\psi}(0) = \frac{1}{2}[\psi(x=0^+) + \psi(x=0^-)], \quad (21)$$

where the delta function potential mentioned is not an exact delta function potential but a point like interaction[20, 21]. The above idea can be deployed at the boundary $x=0$, which leads to the two equations as

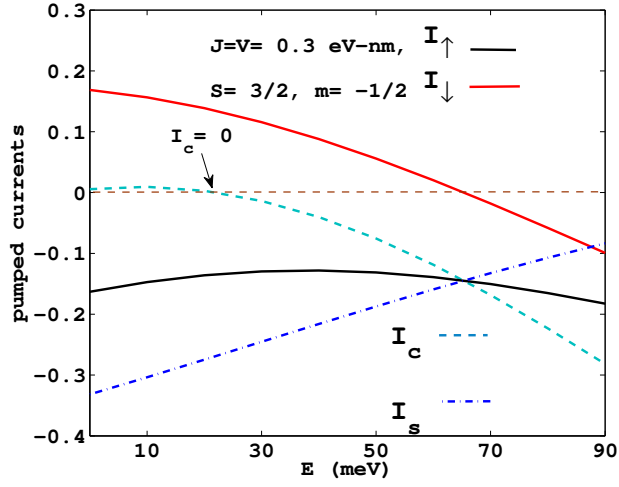
$$\begin{aligned} -i\hbar v_F [\Psi_B^{II}(x=0^+) - \Psi_B^I(x=0^-)] \\ = \frac{J}{2} \vec{s} \cdot \vec{S} [\Psi_A^{II}(x=0^+) + \Psi_A^I(x=0^-)] \end{aligned} \quad (22)$$

$$\begin{aligned} -i\hbar v_F [\Psi_A^{II}(x=0^+) - \Psi_A^I(x=0^-)] \\ = \frac{J}{2} \vec{s} \cdot \vec{S} [\Psi_B^{II}(x=0^+) + \Psi_B^I(x=0^-)] \end{aligned} \quad (23)$$

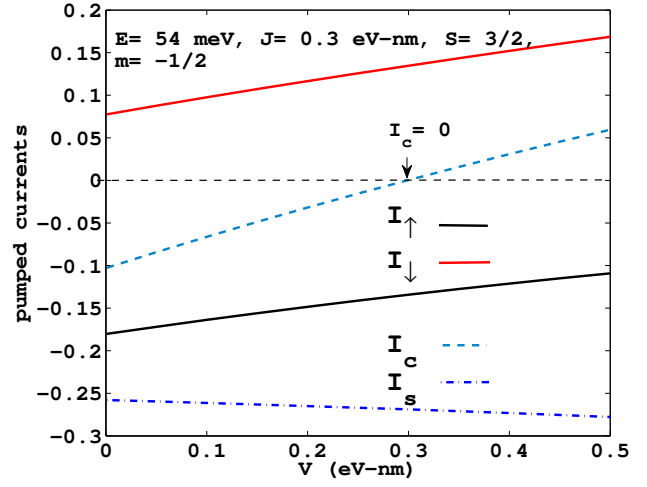
After substituting the wave functions in Eq. (22) and Eq. (23),

$$\begin{aligned} a_{\uparrow}(i\alpha m + e^{i\phi}) + a_{\downarrow}(i\alpha F) + b_{\uparrow}(i\alpha m - e^{-i\phi}) + b_{\downarrow}(i\alpha F) \\ + r_{\uparrow}(i\alpha m + e^{-i\phi}) + r_{\downarrow}(i\alpha F) = e^{i\phi} - i\alpha m, \end{aligned} \quad (24)$$

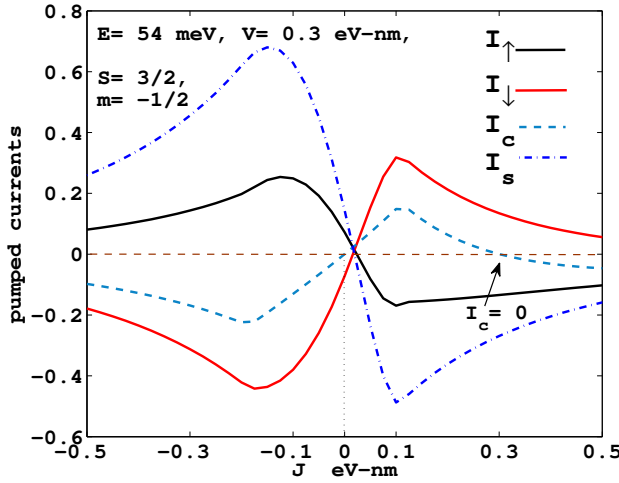
$$\begin{aligned} a_{\uparrow}(i\alpha F) + a_{\downarrow}[e^{i\phi} - i\alpha(m+1)] + b_{\uparrow}(i\alpha F) - b_{\downarrow}[i\alpha(m+1) + e^{-i\phi}] \\ + r_{\uparrow}(i\alpha F) + r_{\downarrow}[e^{-i\phi} - i\alpha(m+1)] = -i\alpha F, \end{aligned} \quad (25)$$



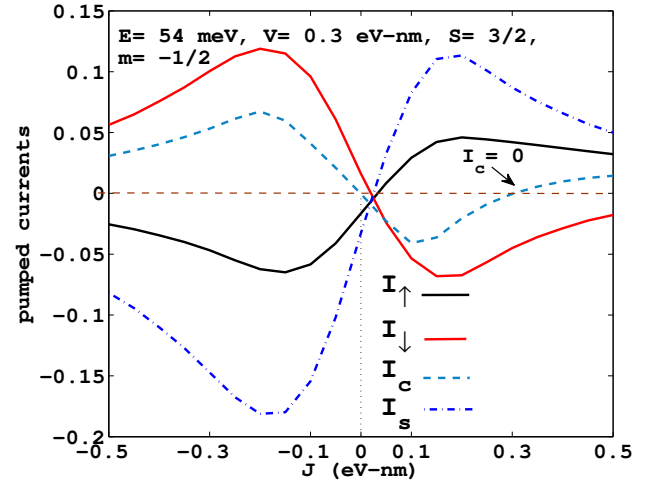
(a) Quantum pumping current Vs. Energy of incident electron for weak pumping



(b) Quantum pumping current Vs. strength of the delta like point interaction for weak pumping



(c) Weak Pumping: Quantum pumping current Vs. Strength of the molecular magnet



(d) Strong Pumping: Quantum pumping current Vs. Strength of the molecular magnet

Figure 2. Pumped spin currents at zero temperature, other parameters are mentioned in Figure.

$$\begin{aligned}
 & a_{\uparrow}(1 + i\alpha m e^{i\phi}) + a_{\downarrow}(i\alpha F e^{i\phi}) + b_{\uparrow}(1 - i\alpha m e^{-i\phi}) - b_{\downarrow}(i\alpha F e^{-i\phi}) \\
 & - r_{\uparrow}(1 + i\alpha m e^{-i\phi}) - r_{\downarrow}(i\alpha F e^{-i\phi}) = 1 - i\alpha m e^{i\phi}, \quad (26)
 \end{aligned}$$

and

$$\begin{aligned}
 & a_{\uparrow}(i\alpha F e^{i\phi}) + a_{\downarrow}[1 - i\alpha(m+1)e^{i\phi}] \\
 & - b_{\uparrow}(i\alpha F e^{-i\phi}) + b_{\downarrow}[1 + i\alpha(m+1)e^{-i\phi}] \\
 & - r_{\uparrow}(i\alpha F e^{-i\phi}) - r_{\downarrow}[1 - i\alpha(m+1)e^{-i\phi}] = i\alpha F e^{i\phi}. \quad (27)
 \end{aligned}$$

Here, $\alpha = J/(2\hbar v_F)$. The mixing of the spin-up and spin-down components in the above equations are attributed to the exchange operator $\mathbf{s} \cdot \mathbf{S}$.

At $x=a$, the boundary conditions are given as:

$$\begin{aligned}
 & -i\hbar v_F [\Psi_B^{III}(x=a^+) - \Psi_B^H(x=a^-)] \\
 & = \frac{V}{2} [\Psi_A^{III}(x=a^+) + \Psi_A^H(x=a^-)]
 \end{aligned}$$

and

$$\begin{aligned}
 & -i\hbar v_F [\Psi_A^{III}(x=a^+) - \Psi_A^H(x=a^-)] \\
 & = \frac{V}{2} [\Psi_B^{III}(x=a^+) + \Psi_B^H(x=a^-)],
 \end{aligned}$$

lead to

$$a_{\uparrow} e^{ika} (iG - e^{i\phi}) + b_{\uparrow} e^{-ika} (iG + e^{-i\phi}) + t_{\uparrow} e^{ika} (e^{i\phi} + iG) = 0, \quad (28)$$

$$a_{\downarrow} e^{ika} (iG - e^{i\phi}) + b_{\downarrow} e^{-ika} (iG + e^{-i\phi}) + t_{\downarrow} e^{ika} (e^{i\phi} + iG) = 0, \quad (29)$$

$$a_{\uparrow} e^{ika} (-1 + iG e^{i\phi}) - b_{\uparrow} e^{-ika} (1 + iG e^{-i\phi}) + t_{\uparrow} e^{ika} (1 + iG e^{i\phi}) = 0, \quad (30)$$

and

$$a_{\downarrow}e^{ika}(-1+iGe^{i\phi})-b_{\downarrow}e^{-ika}(1+iGe^{-i\phi})+t_{\downarrow}e^{ika}(1+iGe^{i\phi})=0, \quad (31)$$

where, $G = V/(2\hbar v_F)$.

The eqns. (24-31) contain 8 unknown probability amplitudes, which can be solved numerically to confirm $|t_{\uparrow}|^2 + |r_{\uparrow}|^2 + |t_{\downarrow}|^2 + |r_{\downarrow}|^2 = 1$. Similarly for the case of spin-down incident electron from the left side, we can get scattering amplitudes. This procedure can be repeated appropriately for spin-up/down electron coming from right side.

III. RESULTS AND DISCUSSIONS

Different components of quantum pumped currents i.e; spin-up (I_{\uparrow}), spin-down (I_{\downarrow}) and net spin current ($I_s = I_{\uparrow} - I_{\downarrow}$) and charge current ($I_c = I_{\uparrow} + I_{\downarrow}$) are obtained numerically using Eq. 12 at zero temperature as shown in figures 2 (a)-(d).

Figure 2(a) and 2(b) show the quantum pumped currents ($I_{\uparrow}, I_{\downarrow}, I_s, I_c$) versus energy of the incident electron (E) and strength of adatom/line defect for weak pumping, without disorder. The following numerical parameters are used (mentioned in the figure also): the spatial separation between SMM and the adatom $a = 10$ nm, the strength of exchange interaction between electron and the molecular magnet $J = 0.3$ eV-nm, $m = -1/2$ and spin of the molecular magnet $S = 3/2$. The strength of line defect potential $V = 0.3$ eV-nm and the strength of the time varying modulations on top of V and J are taken as $x_p = 0.05$ eV-nm in strong pumping case. From figure 2(a), it is seen that for a suitable energy E ($= 54$ meV), the total charge current completely disappears leaving behind a pure spin-current. Fig. 2(b) shows that individual spin pumped currents slowly varying with the increase of ordinary potential. The I_{\uparrow} is decreasing while I_{\downarrow} is increasing with V . The pumped currents in weak pumping regime are in units of I_0 as in Eq. 8, while in strong pumping regime are in units of $ew/2\pi$. Another important point in the weak pumping case is that, by suitably choosing E , I_{\downarrow} can be completely suppressed to pump only I_{\uparrow} a spin up selective current.

Figures 2(c) and 2(d) are plotted to check how the strength of the exchange interaction (J) affects the different pumped currents. We have taken energy of incident electron ($E = 54$ meV) for which pure spin current was observed. From figure 2(c), we see that the pumped currents attain a maximum around $J = 0.1$ and -0.13 eV-nm and then start diminishing towards zero, and pure spin current appears at $J = 0.3$ eV-nm, and spin selective current I_{\downarrow} appears for $J > 0.5$ eV-nm. However, in strong pumping as shown in figure (d), pure spin current appears at the same position at $J = 0.3$ eV-nm. For both weak and strong pumping plots, we have chosen the phase difference between two modulations as $\pi/2$. One important fact which is clearly noticeable is the fact that 'J' acts as a current switch. By changing J from positive to negative, all the pumped currents change sign. This shows that the magnetization of SMM controls the direction of current flow in graphene. Since, we aim to control this by the twist, effectively twisting the SMM changes the direction of spin currents. This is a key result of

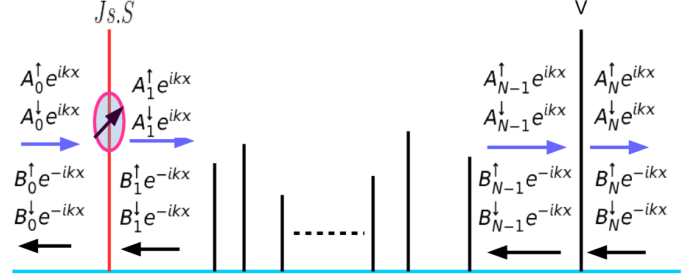


Figure 3. A typical diagram of the disorder added device in which SMM and adatom is separated by a distance a nm.

our work.

A. Effect of Disorder and temperature

In this subsection, we discuss the effects of disorder distributed randomly in the system. We have modeled the present device in such way that SMM and adatom/line defect are at the extreme ends of the sample and disorder is confined between SMM and adatom/line defect. Here each disorder is considered to be a delta potential (point interaction as mentioned before). We solve this problem by using transfer matrix approach. The presence of multiple delta potentials causes a number of confined regions between SMM and the adatom. The general form of the wave function in each region can be written as:

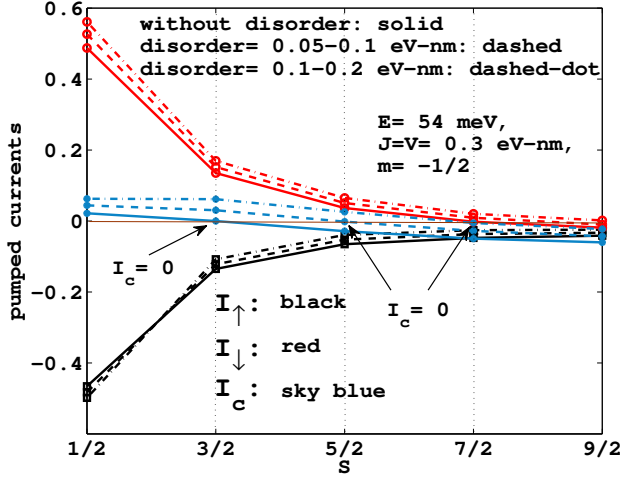
$$\Psi_n(x) = \begin{bmatrix} (A_n^{\uparrow} e^{ikx} + B_n^{\uparrow} e^{-ikx}) \chi_m \\ (A_n^{\downarrow} e^{ikx} + B_n^{\downarrow} e^{-ikx}) \chi_{m+1} \end{bmatrix}. \quad (32)$$

Here $n = 0, 1, 2, 3, \dots, (N-1), N$ corresponding to different regions bounded by the delta potentials, as shown in Fig. 3. The above wave function is for A-sublattice, the phase factor $\exp(\pm i\phi)$ is multiplied with transmission (reflection) amplitude to get the same for B-sublattice. The next step is to find out the total transfer matrix which connects the wave function amplitudes between extreme left and right. To do so, first we find transfer matrix across SMM i.e; between region ' $n = 0$ ' and ' $n = 1$ ' as in Fig. 3,

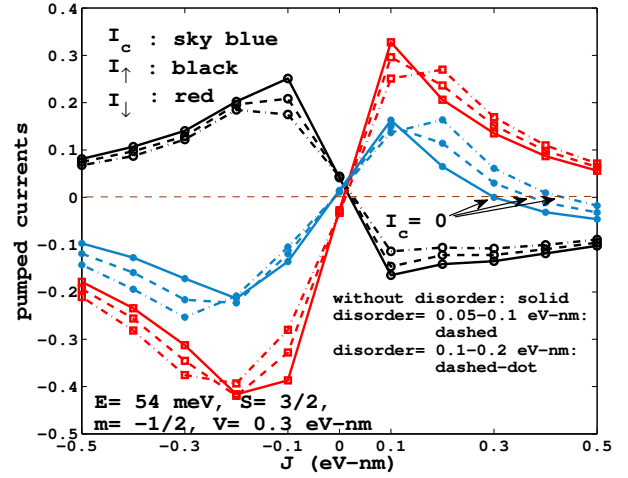
$$\begin{bmatrix} A_1^{\uparrow} \\ A_1^{\downarrow} \\ B_1^{\uparrow} \\ B_1^{\downarrow} \end{bmatrix} = M^{[1,0]} \begin{bmatrix} A_0^{\uparrow} \\ A_0^{\downarrow} \\ B_0^{\uparrow} \\ B_0^{\downarrow} \end{bmatrix}, \quad (33)$$

where $M^{[1,0]}$ is the transfer matrix across SMM, expressed as $M^{[1,0]} = M_1/M_0$ with

$$M_0 = \begin{bmatrix} \xi - igm & -igF & igm - \xi_c & -igF \\ -igF & \xi + ig(m+1) & -igF & -ig(m+1) - \xi_c \\ 1 - igm\xi & -igF\xi & 1 + igm\xi_c & igF\xi_c \\ -igF\xi & 1 + ig(m+1)\xi & igF\xi_c & 1 - ig(m+1)\xi_c \end{bmatrix} \quad (34)$$



(a) Quantum pumped currents in the weak pumping regime vs. spin of the SMM for disordered graphene.



(b) Quantum pumped currents in the weak pumping regime vs. J for disordered graphene.

Figure 4. Pumped spin currents in presence of disorder.

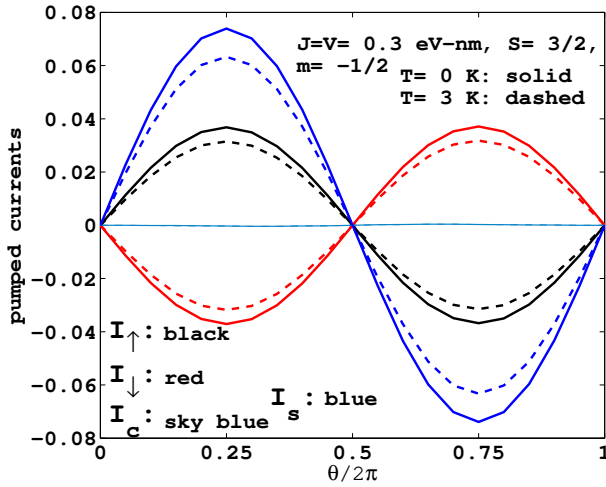


Figure 5. Quantum pumping current Vs. phase angle between two modulations for strong pumping. Solid line is for zero temperature case while dashed line is for finite temperature.

and

$$M_1 = \begin{bmatrix} \xi + igm & igF & igm - \xi_c & igF \\ igF & \xi - ig(m+1) & igF & -ig(m+1) - \xi_c \\ 1 + igm\xi & igF\xi & 1 - igm\xi_c & -igF\xi_c \\ igF\xi & 1 - ig(m+1)\xi & -igF\xi_c & 1 + ig(m+1)\xi_c \end{bmatrix} \quad (35)$$

with $\xi = \exp(i\phi)$ and $\xi_c = \exp(-i\phi)$. Similarly we can get the transfer matrix across any ordinary potential, for example, the

transfer matrix between ' $n = N'$ ' and ' $n = N - 1'$ ' as

$$\begin{bmatrix} A_N^\uparrow \\ A_N^\downarrow \\ B_N^\uparrow \\ B_N^\downarrow \end{bmatrix} = M^{[N,N-1]} \begin{bmatrix} A_{N-1}^\uparrow \\ A_{N-1}^\downarrow \\ B_{N-1}^\uparrow \\ B_{N-1}^\downarrow \end{bmatrix}, \quad (36)$$

where $M^{[N,N-1]}$ is the transfer matrix across adatom, expressed as $M^{[N,N-1]} = M_N/M_{N-1}$ with

$$M_{N-1} = \begin{bmatrix} \xi - iG & 0 & iG - \xi_c & 0 \\ 0 & \xi - iG & 0 & iG - \xi_c \\ 1 - iG\xi & 0 & 1 + iG\xi_c & 0 \\ 0 & 1 - iG\xi & 0 & 1 + iG\xi_c \end{bmatrix} \quad (37)$$

and

$$M_N = \begin{bmatrix} \xi + iG & 0 & iG - \xi_c & 0 \\ 0 & \xi + iG & 0 & iG - \xi_c \\ 1 + iG\xi & 0 & 1 - iG\xi_c & 0 \\ 0 & 1 + iG\xi & 0 & 1 - iG\xi_c \end{bmatrix}. \quad (38)$$

Since the adatom is modeled as a delta function potential and disorder is modeled too as randomly distributed sequence of delta potentials with random strengths the transfer matrix for any arbitrary interface between adatom and SMM has also the same matrix elements as $M^{[N,N-1]}$.

After some straight forward algebra, the connection between the wave function amplitudes of extreme left and right is found to be[20]

$$\begin{bmatrix} A_N^\uparrow \\ A_N^\downarrow \\ B_N^\uparrow \\ B_N^\downarrow \end{bmatrix} = M \begin{bmatrix} A_0^\uparrow \\ A_0^\downarrow \\ B_0^\uparrow \\ B_0^\downarrow \end{bmatrix}, \quad (39)$$

where

$$M = M^{[N,N-1]} M_{free}^{[N-1]} M^{[N-1,N-2]} M_{free}^{[N-2]} \dots M_{free}^{[1]} M^{[1,0]} \quad (40)$$

with M_{free}^n , the propagation matrix between any two successive delta potential, is given by

$$M_{free}^n = \begin{bmatrix} e^{ikd_n} & 0 & 0 & 0 \\ 0 & e^{ikd_n} & 0 & 0 \\ 0 & 0 & e^{-ikd_n} & 0 \\ 0 & 0 & 0 & e^{-ikd_n} \end{bmatrix}. \quad (41)$$

Here, d_n is the separation between two consecutive delta potentials. To calculate the reflection and transmission amplitudes, we shall use the scattering matrix (S-matrix), which is connected to transfer matrix as[20]

$$S = \frac{1}{(M_{22})_{2 \times 2}} \begin{bmatrix} (M_{21})_{2 \times 2} & 1 \\ \det(M) & (M_{12})_{2 \times 2} \end{bmatrix},$$

$$M = \begin{bmatrix} M_{11} & M_{12} \\ M_{21} & M_{22} \end{bmatrix} = \begin{bmatrix} m_{11} & m_{12} & m_{13} & m_{14} \\ m_{21} & m_{22} & m_{23} & m_{24} \\ m_{31} & m_{32} & m_{33} & m_{34} \\ m_{41} & m_{42} & m_{43} & m_{44} \end{bmatrix}. \quad (42)$$

The reflection amplitude (to the left, as we are calculating pumped currents in the left lead)

$$r_l = -\frac{M_{21}}{M_{22}} = \begin{bmatrix} r_{\uparrow\uparrow} & r_{\uparrow\downarrow} \\ r_{\downarrow\uparrow} & r_{\downarrow\downarrow} \end{bmatrix} \quad (43)$$

and transmission amplitude from right to left is

$$t_r = \frac{1}{M_{22}} = \begin{bmatrix} t_{\uparrow\uparrow} & t_{\uparrow\downarrow} \\ t_{\downarrow\uparrow} & t_{\downarrow\downarrow} \end{bmatrix}. \quad (44)$$

The t_r and r_l can be directly used in Eq. (13) to obtain the quantum pumped currents. We must mention here that disorder free pumping current can also be recovered from here by using transfer matrix as $M = M^{[2,1]} M_{free} M^{[1,0]}$, where $M^{[2,1]}$ and $M^{[1,0]}$ would become the transfer matrix across adatom and SMM, respectively.

Disorder effect is shown in Fig. 4(a). Herein we plot the pumped currents as function of the different spin states of SMM in the weak pumping regime. There is pure spin current for $S = 3/2$, in the figure $m = -1/2$. To include disorder, we have chosen the random spacing between any two potentials in the range 1 – 1.5 nm. The strength of the potential is also random and ranges from 50 – 100 meV-nm (dashed line) to 100 – 200 meV-nm (dashed-dot line). We have considered the pumped currents averaged over 1000 realizations. One can see that disorder has a limited effect on the pure spin current. The position of pure spin current is shifted from $S = 3/2$ (without disorder) to $S = 5/2$ (disorder: 50 – 100 meV-nm) and finally $S = 7/2$ (disorder: 100 – 200 meV-nm) however pure spin currents aren't killed off. In Fig. 4b we see the effect of disorder on pumped currents plotted as function of the magnetization of SMM. We again see position of occurrence of pure spin current ($I_c = 0$) changes from $J = 0.3$ to 0.45 eV-nm as one increases disorder. However, disorder has no effect on

magnetization switching of pumped spin currents showing the resilience of the magnetization switching to disorder.

Finally, in figure 5 we plot the pumped currents as function of the phase difference between modulated parameters. We see that pumped current attains maximum at $\theta = \pi/2$ and minima around $\theta = 0, \pi$. The pure spin current is maintained throughout the whole range of θ . The temperature effect is shown in the same figure, which shows a small damping in amplitudes of the individual spin currents. One can see that temperature has no noticeable effect on the pure spin currents apart from a slight diminishing of the magnitude. To conclude this section, pure spin currents in graphene are immune to any temperature increase apart from decrease in magnitude while disorder has a small effect as it shift the parameter regime for occurrence of pure spin currents although it cannot kill it off.

IV. PUMPING VS. RECTIFICATION

A major issue which was flagged right from the early days of quantum pumping was whether the Switkes experiment[5] was a real demonstration of quantum pumping, since the pumped current was observed to be symmetric with respect to Magnetic field reversal just like the two terminal conductance[26]. However since pumped currents are functions of scattering amplitudes and not scattering probabilities they should have no particular symmetry with respect to magnetic field reversal unless the system itself had some particular symmetry[27]. As the Switkes expt. system did not possess any particular symmetry it was quickly recognized that the current attributed as a a pumping current was in effect a rectified current which depend on the Conductance of the system[28]. However there could have been a pumped current which was masked by the rectified currents. The origin of rectified currents is because experimentally at the nanoscale it is difficult to control time varying parameters. Most naturally time varying parameters couple to input and output leads and instead of only pumping a current there is in addition a transport current defined the net conductance through the system. So any quantum pumping at the nanoscale will have rectified currents and therefore it become imperative to have a scheme to differentiate these currents. The rectified spin up current is defined as: $I_{rect} = \frac{w}{2\pi} R \int_S dX_1 dX_2 (C_1 \frac{\partial G_{\uparrow}}{\partial X_1} - C_2 \frac{\partial G_{\uparrow}}{\partial X_2})$, X_i 's are the modulated parameters. In the weak pumping regime we have- $I_{rect} = I_0 (C_1 \frac{\partial G_{\uparrow}}{\partial X_1} - C_2 \frac{\partial G_{\uparrow}}{\partial X_2})$, with $I_0 = we^2 \sin(\theta) \delta X_1 \delta X_2 R / 4\pi^2 \hbar$.

In Fig. 6 We can see clearly that the Conductance (both spin-up as well as spin-down) are symmetric with respect to small values of J . Thus unlike pumped currents whose direction can be changed by changing the magnetization from positive to negative, the conductance on the other hand shows no such effect. The pumped currents are completely asymmetric as function of J as seen in Fig. 2(c) and (d). Thus even if rectified currents will be present in the system the pumped spin current will be distinguished because of their asymmetric nature with respect to magnetization reversal.

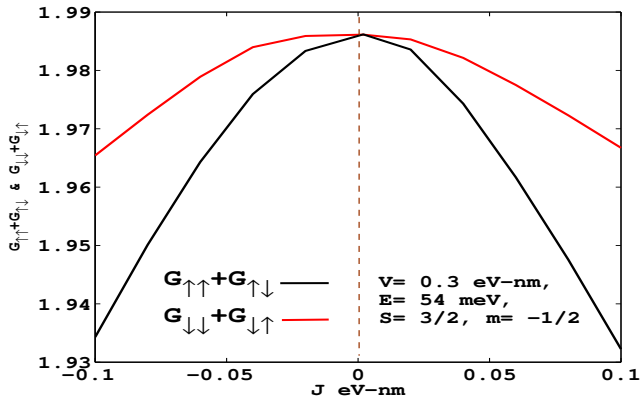


Figure 6. Conductance (spin up and spin down) vs. J . For small J values G 's are symmetric. Compare with Fig 2(c) and (d). Pumped currents up and down spin are asymmetric.

V. EXPERIMENTAL REALIZATION AND CONCLUSIONS

The experimental realization of our pure spin current pumping device shouldn't be too difficult. As already outlined in the last paragraph of the introduction of this paper adiabatically modulating the pressure applied on the single molecule magnet would entail a corresponding adiabatically modulated magne-

tization of SMM. The second adiabatically modulated parameter of the device is an adatom placed "a" distance apart from SMM. The adatom is modeled as a delta function like point interaction similarly embedded in graphene. A gate voltage applied to the adatom can change the potential felt by electrons scattered from it. When the gate voltage itself is adiabatically modulated in time we have all the ingredients for the quantum pumping of pure spin currents and spin selective currents. Alternatively, an extended line defect can be created instead of adatom, which can be controlled experimentally[22–24]. Moreover, one can also use a thin potential barrier experimentally which can be theoretically modeled as a delta like potential. Similarly, the single molecule magnet is in fact a large molecule with host of atoms ranging from 30-100 atoms, these atoms are arranged not only having vertical but also horizontal extension i.e., a single molecule magnet will have sufficient extension along transverse direction. Mention may be made of Ref.29 on single molecule magnets which exemplifies the situation envisaged.

To conclude we have shown that notwithstanding the fact that spin transport via spin orbit effect is almost impossible to be observed in graphene, we have in a novel manner pumped pure spin currents and spin selective currents in graphene via embedding it with a single molecule magnet. The study of pure spin currents in graphene via embedded SMM will be extended to spin correlations and whether one can generate entangled spin currents which will have potential impact on quantum information processing[30] in a subsequent work.

- [1] M. I. Katsnelson, K. S. Novoselov & A. K. Geim, *Nature Physics* 2, 620 - 625 (2006).
- [2] K. S. Novoselov, et. al., *Science*, 315, 1379 (2007); Y. Zhang, et. al., *Nature* 438, 201 (2005).
- [3] R. Inglis, C J Milios, L F Jones, S Piligkos & E K Brechin, 'Twisted molecular magnets' *Chemical Communications*, 48, 181 (2012).
- [4] P. W. Brouwer, *Phys. Rev. B* 58, R10135 (1998).
- [5] M. Switkes, et. al., *Science* 283, 1905 (1999)
- [6] R. Benjamin and C. Benjamin, *Phys. Rev. B* (2004).
- [7] S. K. Watson, R. M. Potok, C. M. Marcus and V. Umansky, *cond-mat/0302492*.
- [8] I. Zutic, J. Fabian, and S. Das Sarma, *Rev. Mod. Phys.* 76, 323(2004).
- [9] N. Tombros, et. al., *Nature* 448, 571 (2007).
- [10] M. H. D. Guimeraes, et. al., *Phys. Rev. B* 90, 235428 (2014).
- [11] M. Popincuc, et. al., *Phys. Rev. B* 80, 214427 (2014).
- [12] Q. Zhang, K. S. Chang and Z. J. Lin, *Appl. Phys. Lett.* 98, 032106 (2011); Q. Zhang, K. S. Chang and Z. J. Lin, *J. Phys.: Condens. Matter* 24, 075302 (2012).
- [13] D. Gatteschi and R. Sessoli, *Angew. Chem. Int. Ed.* 42, 268 (2003).
- [14] W. Wernsdorfer, et. al., *Phys. Rev. B* 65, 180403(R) (2002).
- [15] C. J. Milios, A. Vinslava, P. A. Wood, S. Parsons, W. Wernsdorfer, G. Christou, S. P. Perlepes and E. K. Brechin, *J. Am. chem. Soc.* 129, 8-9 (2007).
- [16] A. Prescimone, C J. Milios, S. Moggach, J E Warren, A R Lennie, J S-Benitez, K. Kamenev, R. Bircher, M. Murie, S. Parsons and E K. Brechin, *Angew. Chem. Int. Ed.* 47, 2828 (2008); E. K. Brechin, Private communication (2015).
- [17] M. Misiorny and J. Barnas, *PRB* 76, 054448 (2007); *Phys. Rev. B* 75, 134425 (2007).
- [18] A. H. Castro Neto, F. Guinea, N. M. R. Peres, K. S. Novoselov, and A. K. Geim *Rev. Mod. Phys.* 81, 109(2009)
- [19] M. Moskalets and M. Buttiker, *Phys. Rev. B* 66, 205320 (2002).
- [20] D J Griffiths and C. A. Steinke, *Amer. J. Phys.* 69, 137 (2001).
- [21] G. Cordourier-Maruri, Y. Omar, R. de Coss, S. Bose, *Phys. Rev. B* 89, 075426 (2014).
- [22] J. Lahiri, et. al., *Nat. Nanotechnol* 5, 326 (2010).
- [23] X. Li, et. al., *J. Am. Chem. Soc.*, 133, 2816 (2011).
- [24] J. H. Chen, et. al., *Phys. Rev. B*, 89, 121407 (R) (2014).
- [25] X-G Li, J. N. Fry and H-P Cheng, *Phys. Rev. B* 90, 125447 (2014).
- [26] P. W. Brouwer, *Phys. Rev. B* 63, 121303(R) (2001)
- [27] T. A. Shutenko, I. Aleiner and B. Altshuler, *Phys. Rev. B* 61, 10366 (2000); I. Aleiner, B. Altshuler and A. Kamenev, *Phys. Rev. B* 62, 10373 (2000).
- [28] Colin Benjamin, *European Physical Journal B* 52, 403 (2006); Colin Benjamin, *Appl. Phys. Lett.* 103, 043120 (2013).
- [29] L. Bogani and W. Wernsdorfer, *Nature materials* 7, 179 (2008).
- [30] Manuscript under preparation.

This figure "disorder.png" is available in "png" format from:

<http://arxiv.org/ps/1506.00754v2>

This figure "flipper.png" is available in "png" format from:

<http://arxiv.org/ps/1506.00754v2>